



HAL
open science

N-Deacetylases required for muramic- δ -lactam production are involved in *Clostridium difficile* sporulation, germination, and heat resistance

Héloïse Coullon, Aline Rifflet, Richard Wheeler, Claire Janoir, Ivo Gomperts Boneca, Thomas Candela

► To cite this version:

Héloïse Coullon, Aline Rifflet, Richard Wheeler, Claire Janoir, Ivo Gomperts Boneca, et al.. N-Deacetylases required for muramic- δ -lactam production are involved in *Clostridium difficile* sporulation, germination, and heat resistance. *Journal of Biological Chemistry*, 2018, 293 (47), pp.18040-18054. 10.1074/jbc.RA118.004273 . hal-04374612

HAL Id: hal-04374612

<https://hal.inrae.fr/hal-04374612>

Submitted on 5 Jan 2024

HAL is a multi-disciplinary open access archive for the deposit and dissemination of scientific research documents, whether they are published or not. The documents may come from teaching and research institutions in France or abroad, or from public or private research centers.

L'archive ouverte pluridisciplinaire **HAL**, est destinée au dépôt et à la diffusion de documents scientifiques de niveau recherche, publiés ou non, émanant des établissements d'enseignement et de recherche français ou étrangers, des laboratoires publics ou privés.



Distributed under a Creative Commons Attribution 4.0 International License

Coullon H.¹, Rifflet A.^{2,3}, Wheeler R.^{2,3}, Janoir C.¹, Boneca I.G.^{2,3} and Candela T.^{1*}

¹EA4043 Unité Bactéries Pathogènes et Santé (UBaPS), Université Paris-Sud, Université Paris-Saclay, 92290 Châtenay-Malabry, France.

²Institut Pasteur, Unité biologie et génétique de la paroi bactérienne, 75724 Paris, France

³INSERM, Équipe Avenir, 75015, Paris

Running title: *Clostridium difficile* spore cortex

*To whom correspondence should be addressed: Thomas Candela: EA 4043–Unité Bactéries Pathogènes et Santé, Université Paris Sud, 92296 Châtenay-Malabry (France)

Thomas.candela@u-psud.fr; Phone : (+33) 1 46 83 53 82 ; Fax : (+33) 1 46 83 55 57

Keywords: *Clostridium difficile*; spore; N-deacetylase; virulence; cortex; germination; sporulation; muramic- δ -lactams

ABSTRACT

Spores are produced by many organisms as the result of a survival mechanism, triggered under several environmental stresses. These are multi-layered structures, one of which is a peptidoglycan layer known as the cortex. This structure contains muramic- δ -lactams that are synthesized by at least two enzymes, CwlD and PdaA. This study focuses on the spore cortex of *Clostridium difficile*, a Gram-positive spore-forming, toxin-producing anaerobic pathogen that can colonize the intestinal tract of humans, considered as the leading cause of antibiotic-associated diarrhea. The cortex of the *C. difficile* 630 Δ erm strain was analyzed using UHPLC coupled to HRMS. This analysis revealed that *C. difficile* cortex differs from *B. subtilis* cortex. Amongst these differences, the muramic- δ -lactams represented 24% in *C. difficile*, compared to 50% in *B. subtilis*. CD630_14300 and CD630_27190 were identified as the genes encoding the *C. difficile* N-deacetylases PdaA1 and PdaA2, responsible for muramic- δ -lactam synthesis. In the *pdaA1* mutant only 0.4% of all muropeptides carry a muramic- δ -lactam modification, and no muramic- δ -lactam were found in the cortex of the double mutant *pdaA1-pdaA2*. Surprisingly, our results suggest a much broader impact for muramic- δ -lactams in *C. difficile* compared to previously characterized model organisms, such

as *B. subtilis*. The *pdaA1* mutant showed a decreased sporulation percentage, an altered germination and a decreased heat-resistance. In a virulence assay, the *pdaA1* mutant also showed a delayed virulence.

C. difficile is a Gram-positive spore-forming, toxin-producing anaerobic bacterium that can colonize the intestinal tracts of humans and other animals (1). *C. difficile* infection (CDI) can lead to a spectrum of clinical signs, ranging from simple self-limiting diarrhea to life-threatening pseudomembranous colitis. Development of the infection have been linked to several risk factors, including antibiotic exposure and compromised immune systems (2). CDI is also associated with recurrent infections, which occur in 20 to 30% of patients who cleared a first infection (2). In healthcare settings, *C. difficile* is considered the leading cause of antibiotic-associated diarrhea (3-5). The increase in cases lead to the classification of *C. difficile* as an emerging infection by the World Health Organization (WHO) in 2009 (6). In fact, hospitalizations for CDI doubled from 2000 through 2010, and an estimated 450 000 cases of CDI occurred in 2011 in the USA. These increased rates and severity of CDI have been speculated to be a consequence of an enhanced *C. difficile* virulence (2,7).

The pathophysiology of CDI is highly dependent on the sporulation and germination ability of *C. difficile*. Contamination results from the ingestion of spores, which can then reach the gastro-intestinal tract. Upon alteration of the host microbiota, spores can germinate and produce vegetative cells. The vegetative cells are then responsible for colonization of the host, production of toxins, and induction of the range of symptoms associated with CDI. Vegetative cells finally sporulate and spores are released in the environment through feces. Spores are therefore both the infectious and the persistence morphotype, responsible for the high dissemination rate of *C. difficile*. It has also been hypothesized that spore persistence in the gastro-intestinal tract is a potential factor in the recurrences and relapses of CDI (2,8). Moreover, a recent study has linked CotE, a spore coat protein, with host colonization, describing the spore as responsible for the initial colonization by targeting and binding the host mucus (9). Through their characteristics and contribution in pathophysiology, spores play a major role in CDI.

Spores are produced by many organisms as the result of a survival mechanism, triggered under several types of adverse environmental conditions. They are one of the most resistant life forms known, able to withstand heat, radiation, chemical exposure, desiccation, as well as treatment with many disinfectants (reviewed in (10)). Such characteristics make for a remarkable persistence ability and contamination potential, and therefore raise concerns in many sectors of human activities, such as the food industry or healthcare, even more so with pathogenic bacteria.

Spores are multi-layered structures, composed of a compressed dehydrated inner core, surrounded by the inner membrane, a germ cell-wall, a peptidoglycan layer known as the cortex, an outer membrane, a proteinaceous external coat, and for some species the outermost layer called the exosporium. Many resistance characteristics of spores have been linked to this specific structural organization (reviewed in (10-12)). Indeed, previous studies

linked the coat with resistance to reactive chemicals such as oxidizing agents and disinfectants (13,14). The dehydration level of the spore core and its high dipicolinic acid (DPA) and small acid-soluble proteins (SASPs) contents has been linked with heat resistance, and DNA protection against radiations and chemical exposure (15). One of the spore specific structures is the thick peptidoglycan layer of the cortex.

The cortex structure has been studied in relatively few organisms, and mostly in *Bacillus*. Structure of the spore cortex has been published for *B. subtilis* (16), and referenced as similar to spore cortex of other *Bacillus* species, such as *B. anthracis*. In *Clostridium* species, two studies analyzed spore cortex composition, using *Clostridium perfringens* and *Clostridium botulinum* (17,18). Spore cortex shows several differences compared to vegetative cell peptidoglycan. In *B. subtilis*, muropeptides of the spore cortex carry either a cyclic muramic acid (muramic- δ -lactam), a tri or tetrapeptide stem, or a single L-Alanine residue, accounting respectively for 50%, 25% and 25% of all muropeptides (16). While muramic- δ -lactams also accounted for nearly 50% of all muropeptides in *C. perfringens*, single L-Alanine residues were not identified in the spore cortex. Instead, tri and tetrapeptide side chains represented over 45% of all muropeptides, and approximately 3% of all muropeptides carried no peptide side chain or δ -lactam ring. Another specificity of spore cortex is a low cross-linking index (11% and 2% in *B. subtilis* (16) and *C. perfringens* (18) respectively) compared to the vegetative cell.

In *B. subtilis*, muramic- δ -lactams have been described to be the result of a three step process (19). The first step is the cleavage of the peptide on a muramic acid by a muramoyl-L-alanine amidase (CwlD) (20), followed by N-deacetylation of the muramic acid by the N-deacetylase PdaA (19). The muramic- δ -lactam ring would then be formed by a transpeptidase. CwlD and PdaA are essential for muramic- δ -lactam synthesis (21). In *B. subtilis*, disruption of any of these enzymes led to the complete disappearance of muramic- δ -lactams in the

cortex, and a strict interruption of the germination process, due to lack of cortex hydrolysis (22). However, mutants lacking either CwID or PdaA are able to produce normal endospores, indicating that muramic- δ -lactam is not required for *B. subtilis* sporulation (22). These enzymes are well described for *B. subtilis* (19,20,23) and *B. thuringiensis* (24), but have yet to be identified in any of the *Clostridium* species and particularly in *Clostridium difficile*.

Given the notable rising concerns in healthcare settings, more and more studies are being conducted on *C. difficile* sporulation-germination mechanisms and host-pathogen interactions. Interestingly, an increasing number of studies have revealed significant differences between *C. difficile* and *B. subtilis* in sporulation and germination (Reviewed in (25-27)). A highly unique structure was described for the vegetative cell peptidoglycan of *C. difficile*, including a high level of N-deacetylation (28) and its impact on host-pathogen interactions. In contrast, we focused on the cortex N-deacetylases. Here, we provide the characterization of CD630_14300, renamed *pdaA1* as the major N-deacetylase responsible for muramic- δ -lactam synthesis in *C. difficile*. Moreover, we also investigated the contribution of cortex structure to *C. difficile* virulence.

Results

C. difficile has an atypical cortex structure

Cortex from pure spore samples were extracted and analyzed through UHPLC (ultra-high-performance liquid chromatography) coupled to HRMS (high-resolution mass spectrometry), as described in material and methods. This analysis of the 630 Δ *erm* spores constitutes the first detailed analysis of the cortex structure of *C. difficile* (Fig 1). The complete list of all mucopeptides detected, their area and calculated relative abundance can be found in Table 1 and Table S1, and the calculated parameters are detailed in Table S2. The vast majority of mucopeptides detected in the analysis of the 630 Δ *erm* parental strain were monomers (90.23% of all mucopeptides), with only 9.77% of dimers and no detectable trimers. These results give a cross-linking index of 4.9%.

Muramic- δ -lactams accounted for 24% of all mucopeptides. While tetrapeptides were the most frequent stem peptide encountered (43.5% of all mucopeptides), the analysis surprisingly showed that 21.9% of mucopeptides were not substituted with a stem peptide of any kind, not even with the single L-Alanine as described in *B. subtilis* (16). The remaining muramic acid residues carried either a tripeptide or dipeptide stem peptide (4.8 and 5.8% respectively). Additionally, 54.7% of mucopeptides were N-deacetylated on the glucosamine residue. Overall, these results suggest that the *C. difficile* spore cortex is different compared to other published cortex analyses.

Identification of the PdaA N-deacetylase candidates

In *B. subtilis*, the N-deacetylase PdaA has been described as responsible for the second step of muramic- δ -lactam synthesis (19). To identify which of the 12 putative N-deacetylases of *C. difficile* were closest to *B. subtilis* PdaA, a multiple alignment was performed using Clustal Omega (29). In these alignments, two potential N-deacetylases of *C. difficile* were the closest to *B. subtilis* PdaA: CD630_14300 and CD630_27190 with 36.7 and 34.7% identity respectively (Table S3). Both *C. difficile* N-deacetylases shared a very high similarity (40.7% identity) with each other and were selected as potential candidates in our study. Using the localization tool PSORT (30), CD630_27190 had a prediction for an internal helix, no signal peptide (PSORT (30)) and a potential membrane lipoprotein lipid attachment site (PROSITE (31)). Given these predictions, the CD630_27190 protein could be membrane associated, either in the vegetative cell membrane, facing the cytoplasm, or in one of the spore membranes. CD630_14300 was predicted to have both an internal helix and a signal peptide, giving a prediction of both cell wall associated and extracellular localization of the protein, which is consistent with a spore cell wall associated protein. To test our hypothesis, CD630_14300 and CD630_27190 were both investigated in *in vitro* experiments.

PdaA1 and PdaA2 are the N-deacetylases responsible for muramic- δ -lactam synthesis

To identify the *B. subtilis* PdaA ortholog in *C. difficile*, the cortex of both mutant strains was analyzed (Table 1, Tables S1 and S2). The CD630_27190 spore cortex was similar to the parental profile, with the exceptions of the appearance of a single N-deacetylated hexasaccharide (peak B, representing 0.21% of all muropeptides), and a slight decrease in N-deacetylation level (49.1% compared to the 54.8% of the parental strain). Other parameters remained similar, including the relative abundance of muramic- δ -lactams.

However, cortex analysis of CD630_14300 mutant spores revealed striking differences relative to the parental cortex. The most notable variation was the disappearance of five peaks, all of which were muropeptides carrying muramic- δ -lactams. Similarly, five additional peaks suffered a strong decrease in relative abundance, producing no detectable precursor ion for fragmentation analysis (grey cells in Table 1). The measured masses (m/z) of these muropeptides were compatible with structures carrying muramic- δ -lactams. Taken together, these variations are responsible for a drastic decrease in muramic- δ -lactam content: only 0.4% of all muropeptides carry a muramic- δ -lactam modification, while 24% of muropeptides carried muramic- δ -lactams in the parental spore cortex. In the CD630_14300 mutant, dimers represented a lower relative amount than in the parental profile (6.20% vs. 9.77%), and the corresponding cross-linking index was decreased in the CD630_14300 mutant (3.10 VS 4.90). Furthermore, the most frequent muropeptides in the CD630_14300 mutant were not the tetrapeptide, as detected in the parental strain, but saccharides carrying neither stem peptide nor muramic- δ -lactam ring. In the CD630_14300 mutant, these muropeptides represented 55.4% of all muropeptides. The CD630_14300 cortex analysis also revealed peaks previously absent from the parental strain, which corresponded to hexasaccharides and octasaccharides carrying various degrees of N-deacetylation. In our analysis, hexasaccharides and octasaccharides

represented a higher relative abundance in the CD630_14300 mutant (11.6% and 5.6% of all muropeptides respectively, compared to 1.80% and 0.10% in the parental strain).

These results suggest that CD630_14300 is the major N-deacetylase responsible for muramic- δ -lactam synthesis, and was therefore renamed *pdaA1*.

The double mutant Δ CD630_14300 Δ CD630_27190 was also constructed. In this mutant, cortex analysis revealed striking differences relative to the parental cortex. The major difference was the total absence of muramic- δ -lactams in the double mutant spore cortex. This result suggest that CD630_27190 is the second N-deacetylase responsible for muramic- δ -lactam synthesis, and was therefore renamed *pdaA2*. As seen with the CD630_14300 mutant, the abundance of unsubstituted muropeptides is increased in the profile obtained for the double mutant (30.7% of all muropeptides, compared to 21.9% for the parental strain).

Spores lacking muramic- δ -lactam undergo a delayed germination

Given the role of muramic- δ -lactam residues in spore germination (22), the *in vitro* germination of *pdaA1* mutant spores was investigated. Spores of the parental 630 Δ erm strain showed a quick OD_{600nm} decrease of about 10% within 10 minutes, followed by a plateau for the remaining 50 minutes (Fig 2A). In comparison, the *pdaA1* mutant showed a slight but reproducible progressive increase in optical density, reaching 3% at 10 minutes. The kinetics of DPA release was also examined and DPA was not released from the spores of the *pdaA1* mutant, in contrast to the parental and the complemented strains (Fig S1A). To assess whether *pdaA1* mutant spores could undergo germination altogether, the monitoring assay was extended to 24 hours (Fig 2B). In this extended monitoring, after 24 hours, parental spores showed a very slow continuous decrease in optical density reaching 80% of the initial OD_{600nm}, and spores lacking PdaA1, showed a slow decrease in OD_{600nm} reaching 90% of the initial OD_{600nm}. In both monitoring assays, the

spores of the *pdaA1* complemented strain showed a profile of optical density similar to the parental spores.

Since colonies of the *pdaA1* mutant were formed after spore plating, germination was investigated using a solid medium incubated for 48h hours. Colonies of the parental and *pdaA1* mutant strains were examined at 24 and 48 hours incubation. Visual examination of both strains showed a strong difference in colony size at 24 hours (Fig 2C-D, Student test, $p=6.6E-11$). Colonies of the parental strain were small but clearly visible (average of 2mm in diameter, Fig 2C), while *pdaA1* colonies were barely visible (average of 1mm). However, colonies no longer showed this difference after 48 hours incubation as both strains had an average diameter of 6mm (Student test, $p=0.99$). These results suggest that *pdaA1* deletion induces a significant delay in germination, but does not block the process altogether. Moreover, in a liquid culture, the *pdaA1* mutant showed no growth defect compared to the parental strain (Fig S2). This result suggests that the colony phenotype observed at 24 hours incubation is further evidence of a germination delay rather than a growth defect. In the complemented mutant, the germination ability is restored (Fig S3). Taken together, the results suggest that the *pdaA1* mutant has an altered germination process.

The germination delay of the double mutant (*pdaA1* and *pdaA2*) was also examined at 24 and 48 hours incubation. Similarly to the phenotype observed for the *pdaA1* mutant, this double mutant is still able to germinate (Fig S3).

Spore morphology of the *pdaA1* mutant

After identifying the cortex modifications and their impact on spore germination, cell morphology was investigated to determine whether such modifications would be associated with an altered spore structure (Fig 3). To allow minimal disruption of spore structures, spore morphology was assessed through transmission electron microscopy (TEM) examination of sporulating cultures obtained with liquid SMC broth and minimal purification steps. Examination of the parental

strain micrographs showed the spore structures as described in (32): an exosporium, the outer and inner coat, outer membrane, cortex, inner membrane and core (Fig 3A). TEM analysis of *pdaA1* mutant spores did not reveal significant differences in spore structure between the parental and *pdaA1* mutant strains (Fig 3A-B). However, for the *pdaA1* mutant spores, the membranes and interfaces of the internal structures appeared blurred and undefined regardless of the focal planes scanned. These observations are particularly visible for the inner and outer membranes. The significance of such a phenotype has yet to be understood.

Overall, examination of sporulating cultures revealed that endospores were less frequent in the *pdaA1* mutant compared to the parental strain (22% vs 55% of cells). Moreover, 79% of *pdaA1* endospores showed an altered morphology (coat detachment or membrane defect), compared to 8% in the parental strain. In addition, the *pdaA1* strain produced a higher amount of debris (Fig S4). Such structures could represent empty spores, detached structures from abnormal spores, or remnants of aborted endospores, suggesting a potential assembly defect in *pdaA1* mutant spores (Fig S4, black arrows).

Modification of cortex structure increases wet heat sensitivity

Since TEM experiments on sporulating cultures suggested a potential anomaly in spore assembly, they were subsequently repeated on pure spore suspensions to allow for measurements and statistical analysis of spore morphology (Fig 4A and Fig S5). While external structures could be focused on, scanning focal planes did not produce clear limitations of internal structures, particularly the membranes and interfaces, as already observed for TEM on sporulating culture. TEM representative images of *C. difficile* spore cross-sections are included in Fig S5 (A-D panels). The results obtained for longitudinal sections can be found in Fig 4A, while full results are detailed in Fig S5 (Table). In longitudinal sections, the core of *pdaA1* mutant spores was longer and wider on average than the parental strain (1122nm and 392.2nm vs

912.9nm and 230.6nm respectively; Student $p < 0.05$). The calculated core volume was three times greater for the *pdaA1* mutant strain compared to the parental strain ($7.39 \times 10^8 \text{nm}^3$ vs $2.08 \times 10^8 \text{nm}^3$, Student $p < 0.05$). The thickness of the cortex layer was also investigated. In the *pdaA1* mutant spore longitudinal cross-sections, the cortex measured an average of 74.54nm, while it only reached 34.17nm for the parental longitudinal cross-sections. These results suggest that the cortex thickness is significantly increased in the *pdaA1* mutant spores, reaching twice the thickness of the parental spore cortex. All the parameters measured and calculated for the longitudinal sections follow a similar trend in the transversal sections (Fig S5). Taken together, these results suggest that *pdaA1* mutant spores are larger, with an increased core volume (3 fold, $p < 0.05$), an increased cortex thickness (2 fold, $p < 0.05$) and a slightly decreased Protoplast/Sporoplast ratio ($p < 0.05$).

After validating the spore assembly and morphology phenotype in the *pdaA1* mutant strain, we sought to identify the potential consequences of such a phenotype on spore resistance characteristics. The chemical resistance of purified *pdaA1* mutant spores was therefore investigated (Fig 4B) as described in (14). Two chemicals, hydrogen peroxide and ethanol, frequently used in chemical resistance spore assays in *C. difficile*, were tested. In our experiments, *pdaA1* mutant spores had a similar log reduction of spore titers after ethanol or hydrogen peroxide treatment compared to the parental and complemented spores (Student test, $p > 0.05$). This result indicates that the defect in spore assembly for the *pdaA1* mutant does not significantly alter the chemical resistance properties of spores. Our results also suggest that ethanol treatment is an appropriate method for enumeration of *pdaA1* mutant spores in sporulating cultures.

Wet heat resistance has been linked to a large number of factors, including factors related to core structure (dehydration, DPA contents, SASPs proteins (10)). Considering that the *pdaA1* mutant spores have an increased core volume compared to the parental strain, which suggests a decreased core dehydration, the heat

resistance of purified *pdaA1* mutant spores was also investigated (Fig 4B). After incubation at 65°C for 20 minutes, spore suspensions of the *pdaA1* mutant strain suffered a greater log reduction compared to the parental and complemented strain (1.15 vs 0.37 and 0.47 logR respectively). This suggests that the heat resistance of *pdaA1* mutant spores is slightly but significantly decreased in comparison with the parental and complemented strain (Student test, $p < 0.05$).

Modification of cortex structure reduces sporulation rate

Since TEM experiment suggested a potential defect in spore assembly, sporulation percentages were investigated for the parental strain harboring the empty control plasmid pMTL84151, the *pdaA1* mutant harboring pMTL84151, and the complemented *pdaA1* mutant harboring pCH67, in sporulating cultures after 72h as described in (33) (Fig 5). Given that the resistance assays indicate that the three strains have a similar resistance to ethanol treatment, enumeration of the relative abundance of spores and vegetative cells was conducted using heat-shock as well as ethanol treatment as a control (Fig 5 A-B). The results of three independent biological replicates can be found for each strain and condition in supporting information (Table S4). Total mean cell titers did not differ between the parental strain harboring the empty pMTL84151 plasmid (2.0×10^6 CFU/mL), the *pdaA1* mutant harboring pMTL84151 (2.3×10^6 CFU/mL), or the *pdaA1* complemented strain harboring the pCH67 plasmid (3.7×10^6 CFU/mL) ($p > 0.05$). In these sporulation studies, ethanol resistant spores represented 37.2% (7.68×10^5 CFU/mL), 6% (1.53×10^5 CFU/mL) and 87.6% (3.11×10^6 CFU/mL) of the total cell titers for the parental strain, the *pdaA1* mutant and the complemented mutant respectively. These results suggest that the *pdaA1* mutant has a reduced sporulation percentage compared to the parental strain ($p < 0.005$). The observed sporulation percentage of the complemented strain suggests that the sporulation defect is restored when complementing the *pdaA1* mutant with pCH67.

Heat resistant spore titers were also counted for the strains, giving rise to different spore counts compared to ethanol treatment. Following 72 hours incubation, spore titers differed in a significant manner for the *pdaA1* mutant: while ethanol resistant spores represented 6% of total cell titers (1.53×10^5 CFU/mL), heat resistant spore titers barely reached 0.13% of total cells (3.8×10^3 CFU/mL). These results indicate that only 2.5% of spores produced by the *pdaA1* mutant are heat resistant (Fig 5B). In comparison, ethanol resistant and heat resistant spores represented 37.2% (5.48×10^5 CFU/mL) and 27.5% (7.68×10^5 CFU/mL) of total cell titers in the parental strain, which indicates that 71% of spores produced at 72h are heat-resistant in the parental strain. Similarly, ethanol resistant and heat resistant spores produced by the complemented strain represented respectively 87% (3.11×10^6 CFU/mL) and 79% (2.86×10^6 CFU/mL) of total cell titers. These results suggest that the *pdaA1* spores have a decreased heat resistance compared to the parental strain ($p < 0.005$), and the phenotype is restored in the complemented strain.

The pdaA1 mutant has a delayed virulence

Since the germination timing of *C. difficile* may modulate the course of the infection process, the ability of the *pdaA1* mutant to cause illness in a hamster model of infection was tested (Fig 6). After oral administration of spores, all hamsters were tested for the presence of *C. difficile* through an on/off detection method, and carriage of *C. difficile* was confirmed for both groups of hamsters. In our assay, all 8 hamsters of the parental strain group were either deceased or euthanized between two and three days post-infection. In comparison, the hamsters infected with *pdaA1* mutant spores survived up to five days post infection before reaching a similar mortality rate. One hamster in this group eventually cleared *C. difficile* from its gastrointestinal tract, and survived throughout the assay (Fig 6A). These results indicate that hamsters infected with the *pdaA1* mutant reached mortality significantly later than those

infected with the parental strain (Fig 6B, $51h \pm 8h$ and $102 \pm 56h$ respectively, $p < 0.05$).

These results indicate that the *pdaA1* mutant has a significantly delayed virulence compared to the parental strain (Kaplan-Meier log rank $p = 0.002286$).

Discussion

Our analysis of *C. difficile* 630 Δ erm spore cortex revealed an atypical structure compared to other species. In our analysis, muramic- δ -lactams were present on 24% of muropeptides, which is significantly less than the relative abundance found in other species (50% in *B. subtilis* and *C. perfringens*). We also determined the glucosamine N-deacetylation level of spore cortex: in the parental 630 Δ erm cortex, approximately 55% of muropeptides are N-deacetylated on the N-acetyl-glucosamine residue (GlcNAc), which constitutes a surprising result in itself, contrasting with the previous published cortex structures (16,18). Indeed, GlcNAc N-deacetylation was not reported at all in *B. subtilis*, and the cortex of *B. megaterium* and *C. perfringens* showed a very low level of GlcNAc N-deacetylation (1% in *B. megaterium* (34), 10% in *C. perfringens* (18)). These differences in cortex N-deacetylation are particularly surprising, given that all these genomes contain several potential N-deacetylases. Indeed, 6 N-deacetylases have been annotated in the *B. subtilis* genome (35). Analysis of *C. perfringens* and *B. megaterium* genomes using the IMG/JGI database (36) showed that these contained 8 and 13 potential N-deacetylases respectively, based on the identification of a pfam01522 domain. Global levels of GlcNAc N-deacetylation in the spore cortex indicates that amongst the remaining potential 11 N-deacetylases of *C. difficile*, there is potentially one enzyme or more able to target this residue in spore cortex, which shows another specificity of *C. difficile* cortex compared to other species. The link between the number of potential N-deacetylases and N-deacetylation levels in spore cortex has yet to be investigated, and to our knowledge the specific impact of GlcNAc N-deacetylation in spore cortex has not been studied in any species. A

first evidence of the N-deacetylase activity on the spore cortex GlcNAc is the slightly decreased N-deacetylation noted in *pdaA2* mutant spore cortex. It is to note that such modification induces no significant difference between the *pdaA2* mutant compared to the parental strain, either in sporulation rate or in germination (Fig S6).

Additionally, our analysis of *C. difficile* cortex also revealed a lack of muropeptides carrying a single L-Alanine (25% of muropeptides in *B. subtilis*), but detected muropeptides carrying no stem peptide or muramic- δ -lactam modification, in a much higher relative abundance than the previous characterization in *C. perfringens* (2.4% of all muropeptides, (18)). In *B. subtilis*, the single L-Alanine muropeptides have been suggested by Popham *et al* (22) to be intermediate states on the pathway to muramic- δ -lactam synthesis, but a precise mechanism has yet to be proposed. Similarly, the small amount of muropeptides carrying a MurNAc with no stem peptide in *C. perfringens* have also been suggested to be the result of intermediate steps of muramic- δ -lactam synthesis (20). In our analysis, these muropeptides carrying no stem peptide or muramic- δ -lactam represent a significantly higher relative abundance than the data published for *C. perfringens* (22% in *C. difficile* vs. 2% in *C. perfringens* (18)). The higher relative abundance of muropeptides carrying a MurNAc with no stem peptide could have an impact on peptidoglycan properties: flexibility, sensitivity to lytic enzymes, protein binding or osmotic properties. These results indicate that *C. difficile* cortex structure is not only highly different compared to *Bacillus* species, but also compared to other *Clostridium* cortex structures published as of today.

In a *C. difficile* mono-associated mice model, *pdaA1* was found to be up-regulated during infection (4.5 fold and 4.1 fold at 14 and 38 h post-challenge respectively (37)), and is suggested to be strongly induced by σ^F and σ^G (38). Moreover, *pdaA1* represents the 14th most abundant mRNA in dormant spores (39). These results suggest that *pdaA1* is expressed both in early and late sporulation stages, with an

increased expression during *in vivo* infection. The cortex analysis of the *pdaA1* mutant significantly differed from that of the 630 Δ *erm* strain. The most striking result was the nearly complete disappearance of muramic- δ -lactams, representing 0.4% of all muropeptides in the *pdaA1* mutant and the complete disappearance in the double mutant *pdaA1-pdaA2* instead of 24% in the 630 Δ *erm* strain. Synthesis of muramic- δ -lactams in *C. difficile* may follow similar steps as described for *B. subtilis*: cleavage by an amidase first (CwlD) (20), followed by N-deacetylation and cyclization of muramic- δ -lactam (19). PdaA1, and to a lesser extend PdaA2, would act as the N-deacetylase in the second step of the synthesis. As observed, their absence would lead to the accumulation of muropeptides carrying no stem peptide or δ -lactam ring (55.4% in the *pdaA1* mutant and 30.7% in the *pdaA1-pdaA2* double mutant vs 21.9% in the parental strain) as the consequence of CwlD cleavage of side-chains. It could be argued that the germination delay of the *pdaA1* mutant is linked to the traces of muramic- δ -lactam still present in the cortex of the *pdaA1* mutant (0.4% of muropeptides). However, the cortex of the *pdaA1-pdaA2* double mutant has a complete lack of muramic- δ -lactams, and spores show a germination delay similar to the *pdaA1* mutant spores. The previous germination delay hypothesis may therefore be discarded.

In *B. subtilis*, lack of muramic- δ -lactams blocked both the cortex hydrolysis and spore outgrowth, and proper germination could only be restored by a lysozyme-induced artificial cortex hydrolysis (20). Surprisingly, lack of muramic- δ -lactams in *C. difficile* does not appear to induce the same interruption of germination. Instead of blocking germination altogether, lack of muramic- δ -lactam in *C. difficile* induced a strongly delayed and slowed germination process, and the artificial cortex hydrolysis was therefore not necessary in our experiments. The most likely hypothesis for such a difference could be that cortex lytic enzymes of *C. difficile* have a less stringent substrate specificity (41,42).

While muramic- δ -lactams have been largely accepted as targets of cortex lytic

enzymes involved in the germination process, the latest studies in *B. subtilis* have linked muramic- δ -lactams with spore outgrowth but not heat resistance or spore dehydration (22). The findings in our study would suggest that muramic- δ -lactams in *C. difficile* spores may play a different role compared to *B. subtilis*. Indeed, in our TEM experiments, spore measurements indicated that while the ultrastructure of spores was globally conserved in the *pdaA1* mutant, lack of muramic- δ -lactams induced an increase in spore volume and cortex thickness, which in turn induced a larger spore. The increase in the heat sensitivity of $\Delta pdaA1$ mutant spores relative to parental spores was not due to decreased DPA levels, since measurement of spore DPA levels revealed that $\Delta pdaA1$ spores had slightly higher levels of DPA than parental spores, without reaching statistically significant values ($P > 0.05$, Fig S1B). Interestingly, the yield of muropeptides from a similar amount of freeze-dried spores in our cortex analysis were comparable for the $630\Delta erm$ and *pdaA1* mutant: similar weight of freeze-dried muropeptides during purification, and similar total peaks area during UHPLC analysis (Table S5), which suggests that the amount of cortex is similar in both strains. This suggests that the difference of thickness between the *pdaA1* mutant and the parental spore cortex may be due to structural differences rather than the amount of peptidoglycan. We hypothesize that, in *C. difficile*, lack of muramic- δ -lactams as a consequence of *pdaA1* deletion could induce a change in spore cortex organization. In turn, this alteration of cortex structure could induce a modification of its physical-chemical properties and may alter the spore dehydration process, giving rise to a larger and more hydrated core. Finally, these alterations would build up to the increased heat sensitivity.

To our knowledge, our study is the first to connect the sporulation process with muramic- δ -lactams. In TEM, our observations noted an increase in abnormal assembly in endospores, associated with the increase in empty round cells and debris. These results are consistent with the empty round cells observed in other studies (33), which have been correlated

to an altered sporulation process. These results are also consistent with the observed sporulation defect of the *pdaA1* mutant (6% vs. 37.1% sporulation percentage respectively). Taken together, our findings suggest that muramic- δ -lactams and their synthesis influence the process of sporulation in *C. difficile*, in contrast with *B. subtilis* for which muramic- δ -lactam deficient spores have been reported to induce no modification of sporulation (22).

In *C. difficile*, mutants affected for germination have either a strongly reduced virulence or no virulence in hamster models. In our study, the *pdaA1* mutant strain has a significant delay in virulence, but eventually reaches a mortality similar to the parental strain. This delay in virulence could be explained by a delayed germination of the *pdaA1* mutant *in vivo*. In Syrian hamsters, *C. difficile* spores have been shown to germinate within the first hour in the small intestine (43). However, spores have been shown to be involved in the first steps of colonization, through adhesion to the host mucus (9). This suggests that *pdaA1* mutant spores may not be fully cleared from the GI tract, and therefore establish infection. However, the delay in germination might change the location in which spores germinate. Among *C. difficile* isolates, lower germination efficiency was correlated to a more severe CDI in mice (44), and the authors suggested that a slight change in germination location within the host may change the severity of the infection. In this study, the potential change in germination location does not alter *C. difficile* virulence.

In CDI, spores are responsible for both infection and dissemination, and intestinal sporulation may have a role in virulence (45). A better sporulation *in vitro* has been correlated to a more severe CDI (46). The *pdaA1* mutant is impaired in sporulation, and may therefore have a lower dissemination rate in the environment and may be less susceptible to promote CDI. N-deacetylase inhibitors are beginning to be investigated (47-50) and one of them may inhibit PdaA1. Inhibiting this N-deacetylase, probably in combination with other potential targets, may allow to reduce sporulation, decrease spore heat resistance, slow germination and therefore

impair *C. difficile* virulence and dissemination capability.

In summary, we showed that muramic- δ -lactams have a much broader impact in *C. difficile* than initially described in *B. subtilis*, and constitute a novel factor linking both the germination and sporulation processes as well as spore heat resistance. Our study adds a significant contribution in the recent efforts to characterize germination and CDI pathogenesis. It provides an insight into a new strategy to target *C. difficile* and its dissemination by targeting enzymes involved in cortex synthesis.

Experimental procedures

Bacterial strains and Plasmids

Plasmids and strains used in this study can be found in Table 2. The *C. difficile* strains are all isogenic derivatives of the 630 Δ *erm* strain (51), an erythromycin-sensitive derivative of the clinical 630 strain (52). *E. coli* was grown aerobically at 37°C in LB medium, supplemented with ampicillin (Amp, 100 μ g/mL), Kanamycin (Kn, 40 μ g/mL), Chloramphenicol (Cm, 25 μ g/mL) as needed. *C. difficile* was routinely grown in brain-heart infusion medium (BHI, BD) sporulation medium (SM, as described in (33)) or SMC medium (39,53). Mutant selection steps of the allelic exchange mutagenesis were carried out on *C. difficile* minimal medium (CDMM, (54)). Media were supplemented with thiamphenicol (Thi, 15 μ g/mL), 0.1% sodium taurocholate (Sigma Aldrich), 1% defibrinated horse blood or “*C. difficile* selective supplement” (25% (w/v) D-cycloserine, 0.8% (w/v) cefoxitin; OXOID) when required. Cultures of *C. difficile* were carried out at 37°C in an anaerobic chamber (Jacomex, 5% H₂ - 5% CO₂ - 90% N₂).

Molecular biology

Plasmid extractions and DNA purifications were carried using the QIAprep spin Miniprep Kit (Qiagen) and E.Z.N.A Cycle Pure Kit (Omega) respectively, according to the manufacturer’s instructions. Polymerase chain reactions (PCR) were carried using either the high fidelity *Phusion* DNA polymerase (Thermo Scientific) for cloning and screening of *C. difficile*, or the Taq DNA Polymerase (New

England Biolabs) from screening steps in *E. coli*. Restriction enzymes were used according the manufacturer’s instructions.

Construction of mutants and complemented strains

Genes of interest were deleted in the 630 Δ *erm* strain using the allelic exchange mutagenesis protocol as described in (55). Plasmids used for the mutagenesis were built using a one-step seamless cloning method, the Circular Polymerase Extension Cloning (56). For each desired mutant, DNA fragments were designed to contain 1200pb sequences of either upstream or downstream of CD630_14300 and CD630_27190 as well as overlapping regions between the vector of choice and DNA fragments (Table S6). These regions were designed to delete the gene of interest, starting from the RBS to the STOP codon. Homologous regions for deletion of CD630_14300 and CD630_27190 were amplified from *C. difficile* 630 Δ *erm* genomic DNA using hybrid primers HC174/HC176 and HC175/HC177, giving rise to two 1220bp DNA fragments. Similarly, homologous regions for CD630_27190 in-frame deletion were amplified using hybrid primers HC185/HC187 and HC186/HC188, giving rise to 1200 and 1230bp DNA fragments. For CPEC cloning, the pMTLSC7315 cloning vector was amplified using 7315A/7315B primers, producing a 6000bp linearized vector. After purification, each set of upstream and downstream DNA fragments were combined with the linearized pMTLSC7315 vector in a 1:1 to 2:1 molar ratio of insert-to-vector, and processed in the specific PCR amplification program recommended in (56,57), producing double stranded circular plasmids that were directly transformed into competent *E. coli* TG1 cells. The two pairs of homologous regions for CD630_14300 and CD630_27190 deletion respectively cloned into the linearized pMTLSC7315 vector gave rise to pMB5 and pMB4. Inserts were sequenced to confirm the absence of mutations in the inserts of both plasmids.

The CD630_14300 and CD630_27190 genes were deleted using allelic exchange

method. The recombinant pMB5 plasmid was transformed into *E. coli* HB101(pRK24) and then introduced into *C. difficile* 630 Δ *erm* strain by heterogramic conjugation, selecting for thiamphenicol resistance. Using the protocol described in (55), single crossover events were screened using HC177/HC178 and HC174/HC179 primer sets. Colonies corresponding to single crossover events were selected, and further processed for selection of the second crossover event. Clones obtained on CDMM medium supplemented with 5-FC were streaked onto BHI and BHI supplemented with Thiamphenicol. Thi^S clones were then screened with HC178/HC179 to detect which clones corresponded to the desired gene deletion. Using these primers, clones producing a 3560bp DNA fragment were considered as parental revertants, and clones producing a 2700bp DNA fragment were isolated and considered as mutants. Similarly, for CD630_27190 deletion, single cross-over events were screened using HC188/HC189 and HC185/HC190, and FC^R Thi^S clones were screened for the second crossover event using HC189/HC190. Clones producing a 3550bp amplification using these primers were considered as parental revertants, and clones producing a 2540bp amplification were isolated and considered as mutants.

To obtain the double mutant Δ CD630_27190, the same method was applied, introducing the deletion of Δ CD630_14300 in the Δ CD630_27190 mutant.

The complementation plasmid for *pdaA1* was built using traditional restriction cloning methods as follows: the full-length sequence of CD630_14300 plus 330bp upstream was PCR amplified from *C. difficile* 630 Δ *erm* genomic DNA using HC254/HC272 (Table S6) and the 1240bp product was ligated into the pBLUNT linear vector from the Zero Blunt PCR Cloning Kit (Invitrogen), giving rise to pCH66. After sequencing, the pCH66 construct and the pMTL84151 definitive vector were digested using *KpnI* and *XbaI*, and the 1.3kb *KpnI/XbaI* DNA sequence extracted from pCH66 was ligated with the linearized pMTL84151, giving rise to the final construct pCH67. The recombinant pCH67 plasmid was transformed

into *E. coli* HB101(pRK24) and then introduced into *C. difficile* Δ *pdaA1* strain by heterogramic conjugation, selecting for thiamphenicol resistance. Similarly, 630 Δ *erm* and Δ *pdaA1* mutant strains received the pMTL84151 empty plasmid as a control.

Spore preparation

Spore preparations for the germination assays, resistance assays, TEM spore measurements and the *in vivo* virulence study were obtained according to an adapted protocol described in (39). Briefly, *C. difficile* was grown 16h in SMC broth, and plated in the morning onto SMC agar plates. Plates were incubated at 37°C in the anaerobic chamber for up to 7 days, monitoring sporulation regularly. Plates were then harvested in water, washed twice and then left at 4°C for 2 to 7 days. Spore suspensions were then washed again with water. When pure spore suspensions were needed, a 20-50% HistoDenz gradient was then applied to the suspensions. To remove traces of HistoDenz, suspensions were then washed an additional 10 times with water, and spore preparations were stored at 4°C. Spore suspension purity was assessed using light microscopy examination as described by Popham *et al* (16). Spore suspensions were considered pure when they were at least 98% free of contaminating vegetative cells, cell debris and sporulating cells.

Transmission electron microscopy

TEM experiments were conducted on two types of spore preparations. Spores and vegetative cells from the sporulating culture were harvested by centrifugation after 48 hours incubation in SMC broth, and washed once in phosphate buffered saline. Spore measurements were obtained using the spore preparation protocol described above. Samples were prepared as described in Sadovskaya *et al.* 2017 (58). Staining and examinations were done by the GABI-MIMA2 TEM Platform at INRA, Jouy-en-Josas, France. Grids were examined with a Hitachi HT7700 electron microscope operated at 80 kV, and images were acquired with a charge-coupled device camera (AMT).

Spore measurements were conducted as follows: 10 longitudinal and 10 transversal spore cross-sections were selected for the parental and *pdaA1* mutant spores. The core length, core width and cortex thickness were measured for each section. The protoplast volume (core), sporoplast volume (core and cortex) were calculated according to Beaman *et al.*: volume = $(4/3) \pi (\text{width}/2) \times 2 \times (\text{length}/2)$ (59). The protoplast-to-sporoplast (P/S) ratio was calculated by dividing the calculated core volume (protoplast) by the volume of the core plus cortex layer (sporoplast).

Spore cortex extraction

Spore cortex extractions were conducted as described in a protocol for *B. subtilis* (16). Briefly, 5mg of freeze-dried pure spore preparations (>99%) were hydrated in water for 16h at 4°C. Suspensions were treated twice with a decoating buffer (50mM TrisHCl pH8, 8M urea, 1% SDS, 50mM DTT) for 1 hour at 37°C. After being washed five times in water, lytic enzymes were inactivated with 5% TCA during 6 minutes at 95°C, spores were washed in Tris-HCl 1M, and then washed five times in water. Spores were then left 16h incubated in a Tris-HCl buffer with trypsin at 37°C. The treated suspensions were then boiled in 1% SDS for 15 minutes. Pellets were washed 15 times with water until total elimination of SDS. Peptidoglycan was then digested 16h with mutanolysin in a sodium phosphate buffer. The suspensions were centrifuged, and muropeptides contained in the supernatant were freeze-dried 16h (Telstar cryodos). Soluble muropeptides were then mixed with an equal volume of 500 mM borate buffer (pH 9) and reduced with sodium borohydride (NaBH₄). After 30 min at room temperature, the pH was adjusted to 3 using orthophosphoric acid (H₃PO₄). After centrifugation, reduced muropeptides were diluted 5-fold in mobile phase (formic acid 0,1% in water).

Muropeptide analysis

Muropeptides were analyzed by UHPLC-HRMS (Unité biologie et génétique de la paroi bactérienne, Institut Pasteur). A Dionex

Ultimate 3000 UHPLC was coupled to a QExactive Focus (ThermoFisher Scientific). Muropeptides were eluted on a Hypersil God C18 aQ (175A, 1.9µm, 2.1x150mm) column. Column temperature was 50°C and the injection volume was 10 µL. UHPLC Gradient was programmed as follows: Solvent A = 0.1% formic acid in Water; Solvent B = 0.1% formic acid in Acetonitrile; Flow = 0.2 mL/min; Run Time = 45 min; gradient 0-15% B in 30 minutes. Mass spectrometry was set to positive ESI mode with a scan range from 200-3000. Full scan data-dependent acquisition selected the top three most abundant precursor ions for tandem mass spectrometry by HCD fragmentation. Peaks were selected with the following criteria: peak area threshold = 2,500 000; at least two fragmentation sets; peak intensity >5000. Percentage of each peak was calculated as the ratio of the peak area over the sum areas of all the peaks in Table 1.

Germination assays

Germination was monitored using an optical density monitoring assay, following a protocol adapted from (60). Biological triplicates were obtained using independent spore preparations, purified as described above. After heat activation at 37°C for 20 minutes, germination was measured by monitoring the decrease in optical density of a purified spore suspension following the addition of 0.1% taurocholate as a germinant. Germination was expressed as the ratio between the OD_{600nm} at a given time and the initial OD_{600nm} of the spore suspension, times 100. In the standard assay, optical density was monitored for an hour. In the extended assay, monitoring was prolonged to 24 hours. Germination was also investigated using a solid medium: spore suspensions were prepared by serial dilution, plated onto BHI agar plates supplemented with horse blood and 0.1% taurocholate and incubated for 48h hours at 37°C in an anaerobic chamber. At 24 and 48 hours incubation, plates of the parental strain and *pdaA1* were photographed, and isolated colonies were measured.

Sporulation and spore resistance assays

Sporulation studies and resistance assays were done according to a slightly modified version of the protocol described in (33). *C. difficile* strains were grown 16h in SM broth containing the appropriate antibiotics, and used to inoculate SM broth to obtain $OD_{600nm}=0.05$. After a 72h incubation at 37°C, 1mL of culture was withdrawn, serially diluted in phosphate-buffered saline.

Total cell titers were calculated by plating 100µl of these untreated dilutions onto BHI plates containing 0.1% taurocholate and the appropriate antibiotics. Ethanol resistant spore titers were calculated by adding an equal volume of absolute ethanol to 400µL of the untreated dilutions, incubating for 15 minutes at room temperature, and finally plating 100µL of alcohol treated dilutions onto plates. Heat resistant spore titers were then calculated by incubating the remaining 400µL of serial dilutions at 65°C for 20 minutes, and then plating 100µL of the appropriate dilutions.

All dilutions were plated onto BHI plates containing taurocholate and the appropriate antibiotics. The percentage of sporulation was determined as the ratio between the number of ethanol resistant cells/mL and the total number of cells/mL times 100. The percentage of heat-resistant spores was determined as the ratio between heat-resistant titers and ethanol-resistant titers times 100.

For the resistance assay on spores, Log reduction was determined as follows: $\log_{10}(\text{Untreated titers}) - \log_{10}(\text{Treated titers})$. Spore suspensions of both the parental strain harboring the empty plasmid, the *pdaA1* mutant harboring the empty plasmid and the complemented *pdaA1* mutant were incubated for 20 minutes at 37°C with 2.5% H₂O₂, 50% ethanol or water as a negative control, followed by serial dilution and plating on BHI agar plates supplemented with 0.1% sodium taurocholate, to allow efficient germination, and the appropriate antibiotics.

In vivo virulence assay

Adult Female Syrian golden hamsters were used for the study. Absence of *C. difficile*

was monitored after reception of animals and before starting the assay. To induce susceptibility to infection with *C. difficile*, hamsters were treated with antibiotics for five days before infection: intraperitoneal injection of clindamycin (0.3mL, 50mg/kg) five days before infection, and oral administration of gentamycin (0.5mL, 2.5mg/kg) twice a day every day for 5 days. Hamsters were infected orally by administration of 5×10^4 spores of either the parental or the *pdaA1* mutant strain. Enumeration of spore suspensions were conducted on solid medium, after 48h incubation at 37°C. *C. difficile* presence was monitored through an on/off test: fecal pellets from each hamster were cultured in BHI supplemented with 0.1% sodium taurocholate for 12 hours, and plated on BHI agar plated supplemented with 25% (w/v) D-cycloserine, 0.8% (w/v) cefoxitin and 1% defibrinated horse blood. Typical fluorescent colonies were screened under UV light (312 nm).

Ethics statement

Adult Female Syrian golden hamsters (95-105g, Charles River France) were housed in individual sterile cages in an animal biosafety level 2 facility within the Central Animal Facility of the Pharmacy Faculty, according to European Union guidelines for the handling of laboratory animals (http://ec.europa.eu/environment/chemicals/lab_animals/home_en.htm) and procedures for infection, euthanasia and specimen collection were approved by the Ethics Committee CAPSUD (Protocol APAFiS #7492-2016101014285698).

Statistics

Statistical analyses, including the Kaplan-Meier survival analysis, were carried out using BiostaTGV (<http://marne.u707.jussieu.fr/biostatgv/?module=tests>), an online statistical analysis service based on calculations obtained with the statistics software R. The P-value is indicated for all comparisons when differences were found to be statistically significant.

Acknowledgements

This work has benefited from the facilities and expertise of MIMA2 MET, INRA - UMR GABI. We thank M. Gohar for his help and support on this project. M. Bleuzé is acknowledged for her technical help in molecular biology.

Conflict of interest: The authors declare that they have no conflicts of interest with the contents of this article

References

1. Rodriguez Diaz, C., Seyboldt, C., and Rupnik, M. (2018) Non-human *C. difficile* Reservoirs and Sources: Animals, Food, Environment. *Advances in experimental medicine and biology* **1050**, 227-243
2. Zanella Terrier, M. C., Simonet, M. L., Bichard, P., and Frossard, J. L. (2014) Recurrent *Clostridium difficile* infections: the importance of the intestinal microbiota. *World journal of gastroenterology* **20**, 7416-7423
3. Cohen, S. H., Gerding, D. N., Johnson, S., Kelly, C. P., Loo, V. G., McDonald, L. C., Pepin, J., and Wilcox, M. H. (2010) Clinical practice guidelines for *Clostridium difficile* infection in adults: 2010 update by the society for healthcare epidemiology of America (SHEA) and the infectious diseases society of America (IDSA). *Infect Control Hosp Epidemiol* **31**, 431-455
4. Debast, S. B., Bauer, M. P., and Kuijper, E. J. (2014) European Society of Clinical Microbiology and Infectious Diseases: update of the treatment guidance document for *Clostridium difficile* infection. *Clin Microbiol Infect* **20 Suppl 2**, 1-26
5. Jones, A. M., Kuijper, E. J., and Wilcox, M. H. (2013) *Clostridium difficile*: a European perspective. *The Journal of infection* **66**, 115-128
6. Lessa, F. C., Winston, L. G., and McDonald, L. C. (2015) Burden of *Clostridium difficile* infection in the United States. *The New England journal of medicine* **372**, 2369-2370
7. Loo, V. G., Poirier, L., Miller, M. A., Oughton, M., Libman, M. D., Michaud, S., Bourgault, A. M., Nguyen, T., Frenette, C., Kelly, M., Vibien, A., Brassard, P., Fenn, S., Dewar, K., Hudson, T. J., Horn, R., Rene, P., Monczak, Y., and Dascal, A. (2005) A predominantly clonal multi-institutional outbreak of *Clostridium difficile*-associated diarrhea with high morbidity and mortality. *The New England journal of medicine* **353**, 2442-2449
8. Deakin, L. J., Clare, S., Fagan, R. P., Dawson, L. F., Pickard, D. J., West, M. R., Wren, B. W., Fairweather, N. F., Dougan, G., and Lawley, T. D. (2012) The *Clostridium difficile* *spo0A* gene is a persistence and transmission factor. *Infection and immunity* **80**, 2704-2711
9. Hong, H. A., Ferreira, W. T., Hosseini, S., Anwar, S., Hitri, K., Wilkinson, A. J., Vahjen, W., Zentek, J., Soloviev, M., and Cutting, S. M. (2017) The Spore Coat Protein CotE Facilitates Host Colonization by *Clostridium difficile*. *The Journal of infectious diseases* **216**, 1452-1459
10. Setlow, P. (2014) Spore Resistance Properties. *Microbiology spectrum* **2**
11. Leggett, M. J., McDonnell, G., Denyer, S. P., Setlow, P., and Maillard, J. Y. (2012) Bacterial spore structures and their protective role in biocide resistance. *Journal of applied microbiology* **113**, 485-498
12. Setlow, P. (2006) Spores of *Bacillus subtilis*: their resistance to and killing by radiation, heat and chemicals. *Journal of applied microbiology* **101**, 514-525
13. Ghosh, S., Setlow, B., Wahome, P. G., Cowan, A. E., Plomp, M., Malkin, A. J., and Setlow, P. (2008) Characterization of spores of *Bacillus subtilis* that lack most coat layers. *Journal of bacteriology* **190**, 6741-6748
14. Permpoonpattana, P., Phetcharaburanin, J., Mikelson, A., Dembek, M., Tan, S., Brisson, M. C., La Ragione, R., Brisson, A. R., Fairweather, N., Hong, H. A., and Cutting, S. M. (2013) Functional characterization of *Clostridium difficile* spore coat proteins. *Journal of bacteriology* **195**, 1492-1503
15. Loshon, C. A., Genest, P. C., Setlow, B., and Setlow, P. (1999) Formaldehyde kills spores of *Bacillus subtilis* by DNA damage and small, acid-soluble spore proteins of the alpha/beta-type protect spores against this DNA damage. *Journal of applied microbiology* **87**, 8-14
16. Popham, D. L., Helin, J., Costello, C. E., and Setlow, P. (1996) Analysis of the peptidoglycan structure of *Bacillus subtilis* endospores. *Journal of bacteriology* **178**, 6451-6458
17. Atrih, A., and Foster, S. J. (2001) Analysis of the role of bacterial endospore cortex structure in resistance properties and demonstration of its conservation amongst species. *Journal of applied microbiology* **91**, 364-372
18. Orsburn, B., Melville, S. B., and Popham, D. L. (2008) Factors contributing to heat resistance of *Clostridium perfringens* endospores. *Applied and environmental microbiology* **74**, 3328-3335
19. Fukushima, T., Yamamoto, H., Atrih, A., Foster, S. J., and Sekiguchi, J. (2002) A polysaccharide deacetylase gene (*pdaA*) is required for germination and for production of muramic delta-lactam residues in the spore cortex of *Bacillus subtilis*. *Journal of bacteriology* **184**, 6007-6015

20. Sekiguchi, J., Akeo, K., Yamamoto, H., Khasanov, F. K., Alonso, J. C., and Kuroda, A. (1995) Nucleotide sequence and regulation of a new putative cell wall hydrolase gene, *cwID*, which affects germination in *Bacillus subtilis*. *Journal of bacteriology* **177**, 5582-5589
21. Gilmore, M. E., Bandyopadhyay, D., Dean, A. M., Linnstaedt, S. D., and Popham, D. L. (2004) Production of muramic delta-lactam in *Bacillus subtilis* spore peptidoglycan. *Journal of bacteriology* **186**, 80-89
22. Popham, D. L., Helin, J., Costello, C. E., and Setlow, P. (1996) Muramic lactam in peptidoglycan of *Bacillus subtilis* spores is required for spore outgrowth but not for spore dehydration or heat resistance. *Proceedings of the National Academy of Sciences of the United States of America* **93**, 15405-15410
23. Fukushima, T., Kitajima, T., and Sekiguchi, J. (2005) A polysaccharide deacetylase homologue, PdaA, in *Bacillus subtilis* acts as an N-acetylmuramic acid deacetylase in vitro. *Journal of bacteriology* **187**, 1287-1292
24. Hu, K., Yang, H., Liu, G., and Tan, H. (2006) Identification and characterization of a polysaccharide deacetylase gene from *Bacillus thuringiensis*. *Canadian journal of microbiology* **52**, 935-941
25. Fimlaid, K. A., and Shen, A. (2015) Diverse mechanisms regulate sporulation sigma factor activity in the Firmicutes. *Current opinion in microbiology* **24**, 88-95
26. Gil, F., Lagos-Moraga, S., Calderon-Romero, P., Pizarro-Guajardo, M., and Paredes-Sabja, D. (2017) Updates on *Clostridium difficile* spore biology. *Anaerobe* **45**, 3-9
27. Paredes-Sabja, D., Shen, A., and Sorg, J. A. (2014) *Clostridium difficile* spore biology: sporulation, germination, and spore structural proteins. *Trends in microbiology* **22**, 406-416
28. Peltier, J., Courtin, P., El Meouche, I., Lemee, L., Chapot-Chartier, M. P., and Pons, J. L. (2011) *Clostridium difficile* has an original peptidoglycan structure with a high level of N-acetylglucosamine deacetylation and mainly 3-3 cross-links. *The Journal of biological chemistry* **286**, 29053-29062
29. Sievers, F., Wilm, A., Dineen, D., Gibson, T. J., Karplus, K., Li, W., Lopez, R., McWilliam, H., Remmert, M., Soding, J., Thompson, J. D., and Higgins, D. G. (2011) Fast, scalable generation of high-quality protein multiple sequence alignments using Clustal Omega. *Molecular systems biology* **7**, 539
30. Yu, N. Y., Wagner, J. R., Laird, M. R., Melli, G., Rey, S., Lo, R., Dao, P., Sahinalp, S. C., Ester, M., Foster, L. J., and Brinkman, F. S. (2010) PSORTb 3.0: improved protein subcellular localization prediction with refined localization subcategories and predictive capabilities for all prokaryotes. *Bioinformatics (Oxford, England)* **26**, 1608-1615
31. de Castro, E., Sigrist, C. J., Gattiker, A., Bulliard, V., Langendijk-Genevaux, P. S., Gasteiger, E., Bairoch, A., and Hulo, N. (2006) ScanProsite: detection of PROSITE signature matches and ProRule-associated functional and structural residues in proteins. *Nucleic acids research* **34**, W362-365
32. Lawley, T. D., Croucher, N. J., Yu, L., Clare, S., Sebahia, M., Goulding, D., Pickard, D. J., Parkhill, J., Choudhary, J., and Dougan, G. (2009) Proteomic and genomic characterization of highly infectious *Clostridium difficile* 630 spores. *Journal of bacteriology* **191**, 5377-5386
33. Pereira, F. C., Saujet, L., Tome, A. R., Serrano, M., Monot, M., Couture-Tosi, E., Martin-Verstraete, I., Dupuy, B., and Henriques, A. O. (2013) The spore differentiation pathway in the enteric pathogen *Clostridium difficile*. *PLoS genetics* **9**, e1003782
34. Atrih, A., Bacher, G., Korner, R., Allmaier, G., and Foster, S. J. (1999) Structural analysis of *Bacillus megaterium* KM spore peptidoglycan and its dynamics during germination. *Microbiology* **145 (Pt 5)**, 1033-1041
35. Fukushima, T., Tanabe, T., Yamamoto, H., Hosoya, S., Sato, T., Yoshikawa, H., and Sekiguchi, J. (2004) Characterization of a polysaccharide deacetylase gene homologue (*pdaB*) on sporulation of *Bacillus subtilis*. *Journal of biochemistry* **136**, 283-291
36. Markowitz, V. M., Chen, I. M., Palaniappan, K., Chu, K., Szeto, E., Grechkin, Y., Ratner, A., Jacob, B., Huang, J., Williams, P., Huntemann, M., Anderson, I., Mavromatis, K., Ivanova, N. N., and Kyrpides, N. C. (2012) IMG: the Integrated Microbial Genomes database and comparative analysis system. *Nucleic acids research* **40**, D115-122
37. Janoir, C., Deneve, C., Bouttier, S., Barbut, F., Hoys, S., Caleechum, L., Chapeton-Montes, D., Pereira, F. C., Henriques, A. O., Collignon, A., Monot, M., and Dupuy, B. (2013) Adaptive strategies and pathogenesis of *Clostridium difficile* from in vivo transcriptomics. *Infection and immunity* **81**, 3757-3769

38. Saujet, L., Pereira, F. C., Serrano, M., Soutourina, O., Monot, M., Shelyakin, P. V., Gelfand, M. S., Dupuy, B., Henriques, A. O., and Martin-Verstraete, I. (2013) Genome-wide analysis of cell type-specific gene transcription during spore formation in *Clostridium difficile*. *PLoS genetics* **9**, e1003756
39. Dembek, M., Stabler, R. A., Witney, A. A., Wren, B. W., and Fairweather, N. F. (2013) Transcriptional analysis of temporal gene expression in germinating *Clostridium difficile* 630 endospores. *PloS one* **8**, e64011
40. Vollmer, W., and Tomasz, A. (2000) The *pgdA* gene encodes for a peptidoglycan N-acetylglucosamine deacetylase in *Streptococcus pneumoniae*. *The Journal of biological chemistry* **275**, 20496-20501
41. Heffron, J. D., Sherry, N., and Popham, D. L. (2011) In vitro studies of peptidoglycan binding and hydrolysis by the *Bacillus anthracis* germination-specific lytic enzyme SleB. *Journal of bacteriology* **193**, 125-131
42. Wu, X., Grover, N., Paskaleva, E. E., Mundra, R. V., Page, M. A., Kane, R. S., and Dordick, J. S. (2015) Characterization of the activity of the spore cortex lytic enzyme CwlJ1. *Biotechnology and bioengineering* **112**, 1365-1375
43. Wilson, K. H., Sheagren, J. N., and Freter, R. (1985) Population dynamics of ingested *Clostridium difficile* in the gastrointestinal tract of the Syrian hamster. *The Journal of infectious diseases* **151**, 355-361
44. Carlson, P. E., Jr., Walk, S. T., Bourgis, A. E., Liu, M. W., Kopliku, F., Lo, E., Young, V. B., Aronoff, D. M., and Hanna, P. C. (2013) The relationship between phenotype, ribotype, and clinical disease in human *Clostridium difficile* isolates. *Anaerobe* **24**, 109-116
45. Dembek, M., Willing, S. E., Hong, H. A., Hosseini, S., Salgado, P. S., and Cutting, S. M. (2017) Inducible Expression of *spoOA* as a Universal Tool for Studying Sporulation in *Clostridium difficile*. *Front Microbiol* **8**, 1793
46. Carlson, P. E., Jr., Kaiser, A. M., McColm, S. A., Bauer, J. M., Young, V. B., Aronoff, D. M., and Hanna, P. C. (2015) Variation in germination of *Clostridium difficile* clinical isolates correlates to disease severity. *Anaerobe* **33**, 64-70
47. Ariyakumaran, R., Pokrovskaya, V., Little, D. J., Howell, P. L., and Nitz, M. (2015) Direct Staudinger-Phosphonite Reaction Provides Methylphosphonamidates as Inhibitors of CE4 De-N-acetylases. *Chembiochem* **16**, 1350-1356
48. Chibba, A., Poloczek, J., Little, D. J., Howell, P. L., and Nitz, M. (2012) Synthesis and evaluation of inhibitors of *E. coli* PgaB, a polysaccharide de-N-acetylase involved in biofilm formation. *Org Biomol Chem* **10**, 7103-7107
49. Hall, R. S., Brown, S., Fedorov, A. A., Fedorov, E. V., Xu, C., Babbitt, P. C., Almo, S. C., and Raushel, F. M. (2007) Structural diversity within the mononuclear and binuclear active sites of N-acetyl-D-glucosamine-6-phosphate deacetylase. *Biochemistry* **46**, 7953-7962
50. Murphy-Benenato, K. E., Olivier, N., Choy, A., Ross, P. L., Miller, M. D., Thresher, J., Gao, N., and Hale, M. R. (2014) Synthesis, Structure, and SAR of Tetrahydropyran-Based LpxC Inhibitors. *ACS medicinal chemistry letters* **5**, 1213-1218
51. Hussain, H. A., Roberts, A. P., and Mullany, P. (2005) Generation of an erythromycin-sensitive derivative of *Clostridium difficile* strain 630 (630Deltaerm) and demonstration that the conjugative transposon *Tn916DeltaE* enters the genome of this strain at multiple sites. *Journal of medical microbiology* **54**, 137-141
52. Sebahia, M., Wren, B. W., Mullany, P., Fairweather, N. F., Minton, N., Stabler, R., Thomson, N. R., Roberts, A. P., Cerdano-Tarraga, A. M., Wang, H., Holden, M. T., Wright, A., Churcher, C., Quail, M. A., Baker, S., Bason, N., Brooks, K., Chillingworth, T., Cronin, A., Davis, P., Dowd, L., Fraser, A., Feltwell, T., Hance, Z., Holroyd, S., Jagels, K., Moule, S., Mungall, K., Price, C., Rabinowitsch, E., Sharp, S., Simmonds, M., Stevens, K., Unwin, L., Whithead, S., Dupuy, B., Dougan, G., Barrell, B., and Parkhill, J. (2006) The multidrug-resistant human pathogen *Clostridium difficile* has a highly mobile, mosaic genome. *Nature genetics* **38**, 779-786
53. Permpoonpattana, P., Hong, H. A., Phetcharaburanin, J., Huang, J. M., Cook, J., Fairweather, N. F., and Cutting, S. M. (2011) Immunization with *Bacillus* spores expressing toxin A peptide repeats protects against infection with *Clostridium difficile* strains producing toxins A and B. *Infection and immunity* **79**, 2295-2302

54. Cartman, S. T., and Minton, N. P. (2010) A mariner-based transposon system for in vivo random mutagenesis of *Clostridium difficile*. *Applied and environmental microbiology* **76**, 1103-1109
55. Cartman, S. T., Kelly, M. L., Heeg, D., Heap, J. T., and Minton, N. P. (2012) Precise manipulation of the *Clostridium difficile* chromosome reveals a lack of association between the *tcdC* genotype and toxin production. *Applied and environmental microbiology* **78**, 4683-4690
56. Quan, J., and Tian, J. (2011) Circular polymerase extension cloning for high-throughput cloning of complex and combinatorial DNA libraries. *Nature protocols* **6**, 242-251
57. Quan, J., and Tian, J. (2014) Circular polymerase extension cloning. *Methods in molecular biology (Clifton, N.J.)* **1116**, 103-117
58. Sadvskaya, I., Vinogradov, E., Courtin, P., Armalyte, J., Meyrand, M., Giaouris, E., Palussiere, S., Furlan, S., Pechoux, C., Ainsworth, S., Mahony, J., van Sinderen, D., Kulakauskas, S., Guerardel, Y., and Chapot-Chartier, M. P. (2017) Another Brick in the Wall: a Rhamnan Polysaccharide Trapped inside Peptidoglycan of *Lactococcus lactis*. *mBio* **8**
59. Beaman, T. C., Greenamyre, J. T., Corner, T. R., Pankratz, H. S., and Gerhardt, P. (1982) Bacterial spore heat resistance correlated with water content, wet density, and protoplast/sporoplast volume ratio. *Journal of bacteriology* **150**, 870-877
60. Donnelly, M. L., Fimlaid, K. A., and Shen, A. (2016) Characterization of *Clostridium difficile* Spores Lacking Either SpoVAC or Dipicolinic Acid Synthetase. *Journal of bacteriology* **198**, 1694-1707
61. Heap, J. T., Pennington, O. J., Cartman, S. T., and Minton, N. P. (2009) A modular system for *Clostridium* shuttle plasmids. *Journal of microbiological methods* **78**, 79-85
62. Glauner, B., Holtje, J. V., and Schwarz, U. (1988) The composition of the murein of *Escherichia coli*. *The Journal of biological chemistry* **263**, 10088-10095

Footnotes

This study has received funding from the French Government's Investissement d'Avenir program, Laboratoire d'Excellence "Integrative Biology of Emerging Infectious Diseases" (grant n°ANR-10-LABX-62-IBEID). HC was funded by MESR.

The abbreviations used are: TEM, transmission electron microscopy; CDI, *Clostridium difficile* infection; BHI, Brain Heart Infusion; CDMM, *Clostridium difficile* minimal medium; SM, sporulation medium; SMC, sporulation medium C; LB, Luria Bertani; Kn, Kanamycin; Cm, Chloramphenicol; Thi, Thiamphenicol; DTT, dithiothreitol; SDS, sodium dodecyl sulfate; TCA, Trichloro acetic acid; CFU, colony forming unit; GlcNAc, *N*-Acetyl-glucosamine; MurNAc, *N*-Acetylmuramic acid ; RT, retention time; deAc, *N*-deacetylation; ND, not detected; NI, not identified; SASPs, small acid-soluble proteins; UHPLC-HRMS, ultra-high-performance liquid chromatography–high-resolution mass spectrometry; CPEC, circular polymerase extension cloning, DPA, dipicolinic acid.

Table 1. Muropeptides detected in the cortex analysis of 630 Δ erm, Δ CD630_14300, Δ CD630_27190 and Δ CD630_14300 Δ CD630_27190 strains

Peak	Muropeptide	RT	Expected m/z	Measured m/z	Percentages			
					630 Δ erm	Δ CD14300	Δ CD27190	Δ CD14300 Δ CD27190
1	Tetrapeptide missing GM	2.28	462.21945	462.21945	9.47	3.92	4.98	0.13
2	Tetrasaccharide (open lactam) deAc	2.42	440.20006	440.2002	0.74	0.02	0.39	ND
3	Tetrasaccharide (Reduced muramic lactam) deAc	2.77	431.19478	431.19531	6.49	0.25	4.04	ND
4	GM	3.4	499.21337	499.21387	8.25	9.69	10.81	1.49
5	Tetrasaccharide (Open lactam)-Tetrapeptide deAcX2	3.62	427.53282	427.53366	0.92	ND	1.23	ND
6	GMTriptide deAc	3.93	415.1864	415.1881	0.55	0.27	0.96	2.48
7	Tetrasaccharide (Open lactam)	4.26	461.20534	461.20618	0.75	0.03	1.47	ND
8	GMTetrapeptide Gly	4.6	443.6980	443.6985	0.96	0.41	0.69	1.00
9	Tetrasaccharide (Reduced muramic lactam)-Tetrapeptide deAcX2	4.72	421.52929	421.52951	5.92	0.04	4.61	ND
10	Tetrasaccharide (Reduced muramic lactam)	4.72	452.20006	452.2003	5.27	0.24	5.55	ND
11	Tetrasaccharide deAc	5.91	468.19498	468.19614	0.82	6.76	1.15	2.02
12	GMDipeptide deAc	6.65	657.2811	657.28381	2.28	3.94	2.79	3.11
13	GMTetrapeptide deAc	7.38	450.70585	450.70566	16.01	13.66	14.30	17.49
14	Tetrasaccharide (Reduced muramic lactam)- Tetrapeptide deAc	7.47	652.79559	652.79578	19.08	0.06	17.98	ND
15	Hexasaccharides deAcX2	7.96	686.27963	686.28064	0.18	3.11	0.28	1.01
16	Octasaccharides deAcX3	8.71	603.2453	603.2463	0.09	1.62	0.13	0.42
17	GMDipeptide	8.92	699.29307	699.29486	2.62	3.05	3.37	2.83
18	GMTetrapeptide	9.4	471.7102	471.7119	2.56	4.22	3.58	8.93
19	Tetrasaccharide	9.53	489.20026	489.202	1.35	8.28	2.32	5.15
20	Tetrasaccharide-Tetrapeptide deAcX2	9.89	446.19609	446.1976	1.09	7.16	0.49	7.57
A	Tetrasaccharide-Dipeptide deAcX2	10.07	547.22955	547.23035	ND	1.56	ND	1.29
21	Tetrasaccharide (Reduced muramic lactam)- Tetrapeptide	10.37	673.8009	673.8033	2.40	0.02	3.41	ND
22	Tetrasaccharide (Reduced muramic lactam)-Dipeptide	10.53	552.2399	552.2419	0.62	ND	0.94	ND
23	Hexasaccharide (Reduced muramic lactam)_01	10.52	691.29	691.2933	0.64	0.15	1.05	ND
B	Hexasaccharides deAc_01	10.66	707.28491	707.2856	ND	1.82	0.21	0.85
24	Tetrasaccharide-Tetra deAc_01	10.76	689.7958	689.7961	0.00	2.51	0.00	5.93
25	Hexasaccharide (Reduced muramic lactam)_02	10.84	691.29	691.2933	0.80	ND	1.15	ND
26	NI	10.89	ND	729.6561	0.19	ND	0.21	ND
C	Octasaccharides deAcX2_01	11.17	617.2488	617.24921	ND	3.17	ND	0.67
D	Hexasaccharides deAc_02	11.31	707.28491	707.28601	ND	5.94	ND	2.06
27	NI	11.35		729.6561	0.25	ND	0.29	ND
E	Octasaccharides deAcX2_02	11.55	925.3696	925.3709	ND	0.50	ND	0.35
28	Tetrasaccharide-Tetrapeptide deAc_02	11.98	689.79578	689.7987	0.73	9.85	1.47	12.08
F	NI	12.27		815.326	ND	0.87	ND	ND
29	Tetrasaccharide-Tetrapeptide	12.81	710.80106	710.8016	0.16	0.97	0.49	4.95
30	GMTriptide + GMTetrapeptide deAcX2_01	12.88	570.922	570.92438	3.22	1.98	3.92	5.27
31	Tetrasaccharide-Tetrapeptide + GMTriptide deAcX3_01	13.15	537.48625	537.4879	0.55	0.38	0.47	0.47
32	GMTriptide + GMTetrapeptide deAcX2_02	13.49	570.92281	570.92517	2.97	1.31	3.12	3.87
33	GMTetrapeptide + GMTetrapeptide deAcX2	13.58	594.60185	594.6047	0.34	0.37	0.36	0.83
34	Tetrasaccharide-Tetrapeptide + GMTri peptide deAcX3_02	13.68	537.48625	537.4879	0.45	0.22	0.36	0.38
35	GMTriptide + GMTetrapeptide deAc_01	13.85	876.8867	876.8891	0.26	0.40	0.29	0.99
36	GMTetrapeptide + GMTetrapeptide deAcX2_02	14.11	594.60185	594.6047	0.38	0.36	0.39	0.77
37	GMTriptide + GMTetrapeptide deAc_02	14.48	876.88586	876.8891	0.15	0.11	0.16	0.50
38	Tetrasaccharide-Tetrapeptide + GMTriptide deAcX2_01	14.68	730.3161	730.3197	0.29	0.51	0.34	0.85
39	GMTriptide + GMTetrapeptide	15.08	897.89114	897.8958	0.03	0.13	0.05	0.32
40	Tetrasaccharide-Tetrapeptide+ GMTri peptide deAcX2_02	15.21	730.3161	730.3197	0.17	0.14	0.20	0.41

Δ CD14300, CD630_14300; Δ CD27190, CD630_27190 cortex; GM, GlcNAc-MurNAc; RT, retention time; deAc, N-deacetylation of the glucosamine; deAcX2, number of N-deacetylated glucosamine; Tri, disaccharide-tripeptide; Tetra, disaccharide-tetrapeptide; Gly, glycine; ND, not detected in the profile; NI, not identified with the fragmentation profile; grey cells, peaks for which precursor ion was not abundant enough to allow for fragmentation. Tri and tetra contain E-mDAP. The charge z is indicated in Table S1. Percentage of each peak was calculated as the ratio of the peak area over the sum of areas of all the peaks identified in the table.

Table 2. Strains and plasmids

Name	Characteristics	Reference
Bacterial strains		
<i>Escherichia coli</i>		
TG1	<i>E. coli</i> k12 (F', <i>tra</i> D36, <i>lacIq</i> , Δ <i>lacZ</i> , MIS, <i>pro</i> A+B+/SupE, Δ (<i>hdsM-mcrB</i>))	Laboratory
HB101pRK24	<i>E. coli</i> (pRK24) (F - Δ (<i>gpt-proA</i>) 62 Leu B6 <i>gln</i> V44 <i>ara</i> -14 <i>galK2 lacY1</i> Δ (<i>mcrC-mrr</i>) <i>rps</i> L20 (<i>srf'</i>) <i>xyl</i> -5 <i>mlt</i> -1 <i>rec</i> A13, pRK24)	Laboratory
<i>Clostridium difficile</i>		
630 Δ <i>erm</i>	Erythromycin sensitive 630 derived strain	(51)
630 Δ <i>erm</i> Δ 14300, <i>pdaA1</i> mutant	Δ CD630_14300 derivative of 630 Δ <i>erm</i> strain	This work
630 Δ <i>erm</i> Δ 27190, <i>pdaA2</i> mutant	Δ CD630_27190 derivative of 630 Δ <i>erm</i> strain	This work
630 Δ <i>erm</i> Δ 27190 Δ 14300	Δ CD630_14300 derivative of 630 Δ <i>erm</i> Δ 27190 (<i>pdaA2</i>) mutant	This work
630 Δ <i>erm</i> (pMTL84151)	630 Δ <i>erm</i> strain carrying the empty control plasmid pMTL84151	This work
630 Δ <i>erm</i> Δ 14300(pMTL84151)	Δ <i>pdaA1</i> mutant strain carrying the empty control plasmid pMTL84151	This work
630 Δ <i>erm</i> Δ 14300(pCH67)	Δ <i>pdaA1</i> mutant strain carrying the complementation plasmid pCH67	This work
Plasmids and vectors		
pBLUNT	Linear cloning vector, blunt extremities, <i>lacA</i> α - <i>ccdB</i> , MCS,T7 promotor, kanamycin resistance, pUC origin	Invitrogen
pMTL-SC7315	Circular cloning vector, 6000 nucleotides, <i>catP</i> , <i>codA</i> ,	(55)
pMTL-84151	Circular cloning vector, 6300 nucleotides, <i>catP</i> , <i>aLacZ</i> .	(61)
pMB4	pMTLSC7315 derived CPEC assembly of homologous regions for the deletion of CD630_27190	This work
pMB5	pMTLSC7315 derived CPEC assembly of homologous regions for the deletion of CD630_14300	This work
pCH66	pBLUNT derived traditional cloning of insert 94 for <i>pdaA1</i> complementation	This work
pCH67	pCH66 subcloning for <i>pdaA1</i> complementation, pMTL84151 derived	This work

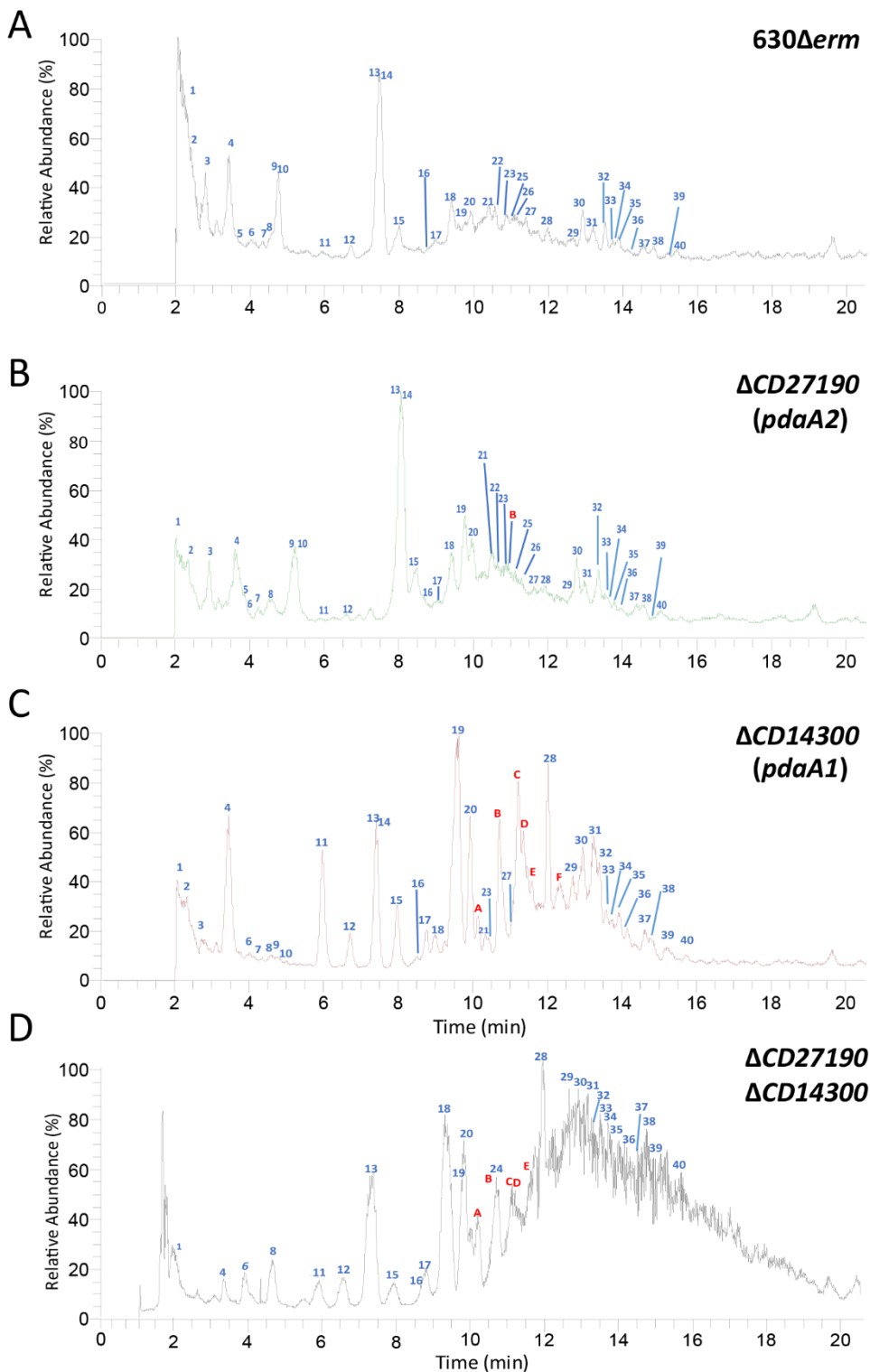


Figure 1. Muropeptide analysis of spore peptidoglycan by HRMS coupled UHPLC. Relative abundance (%) of muropeptides for the 630 Δ erm strain (A), Δ CD630_27190 (B), Δ CD630_14300 (C) and double Δ CD630_14300 Δ CD630_27190 (D) mutants. Numerical peaks refer to peaks identified in the parental strain. Alphabetical peaks refer to new peaks identified in the mutant profiles. Peak identification refers to Table 1.

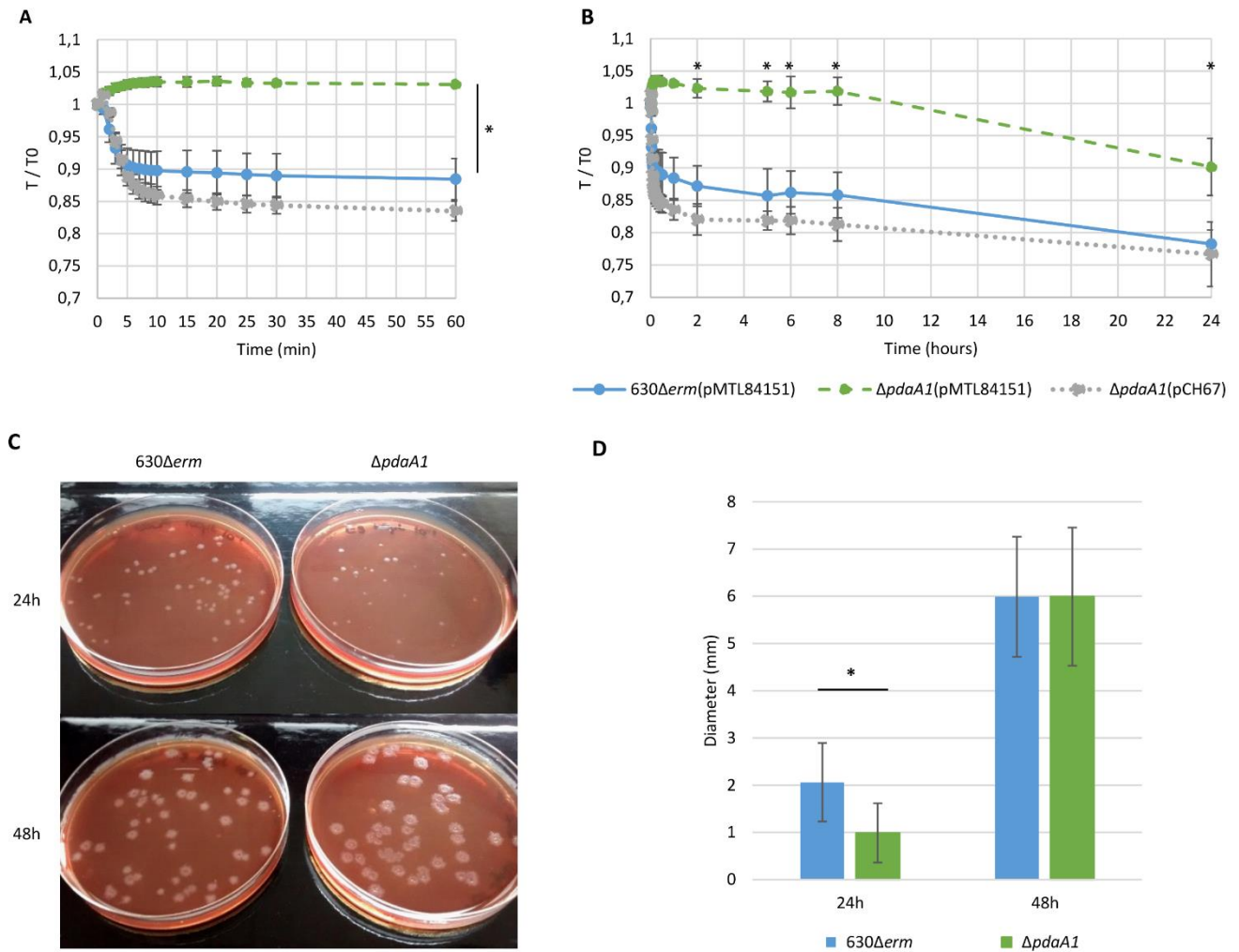


Figure 2. Spores lacking muramic- δ -lactam undergo a delayed germination

Spore germination was monitored for the optical density assay at 600nm after the addition of 0.1% sodium taurocholate in BHISG, for 60 minutes (A) or 24h (B), for the 630Δerm(pMTL84151) parental strain in blue, ΔpdaA1(pMTL84151) strain in green and the complemented pdaA1 mutant strain (ΔpdaA1(pCH67)) in grey. Results are expressed as the ratio of OD_{600nm} observed at time point (T) over the initial OD_{600nm} at T=0 (T₀). Assessment of germination delay in solid BHI supplemented with horse blood and taurocholates was performed for the 630Δerm and the ΔpdaA1 strains (C). Colony sizes were measured (D) and presented in blue for the 630Δerm strain and in green for the ΔpdaA1 strain. * Student test, $p < 0.005$. Results are expressed as the average values and standard deviations of at least three independent experiments, except for the assessment of germination delay in solid BHI (C) which is representative of three independent experiments.

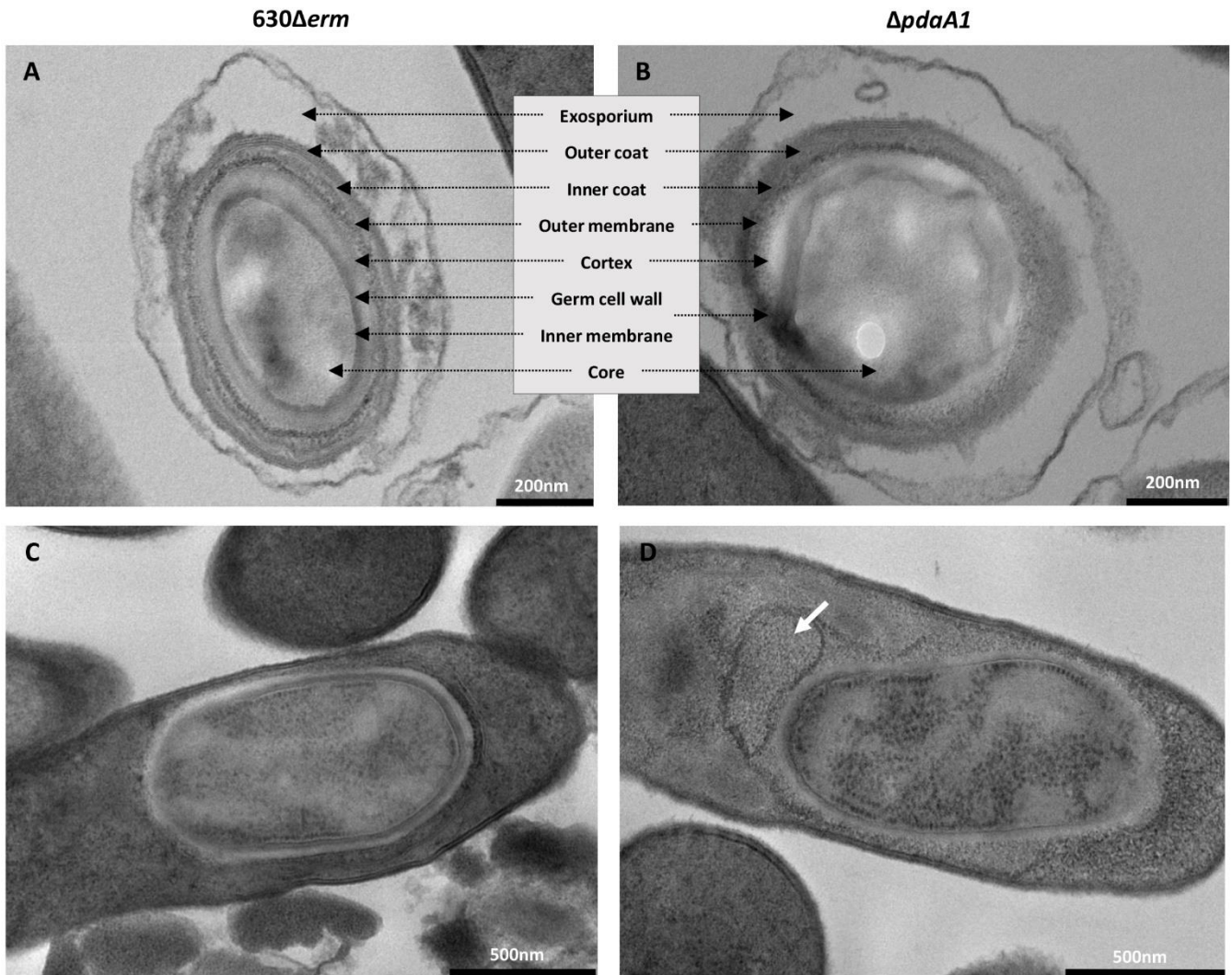


Figure 3. *pdaA1* mutant spore morphology

Electron microscopy of 630 Δ *erm* spores (A) and endospores (C), compared to Δ *pdaA1* mutant spores (B) and endospores (D). The spores layers identified are indicated in the insert between A and B. The legends are indicated by the bars in the bottom right corner, representing 200nm for the spores, and 500nm for the endospores. The white arrow indicate detached structures.

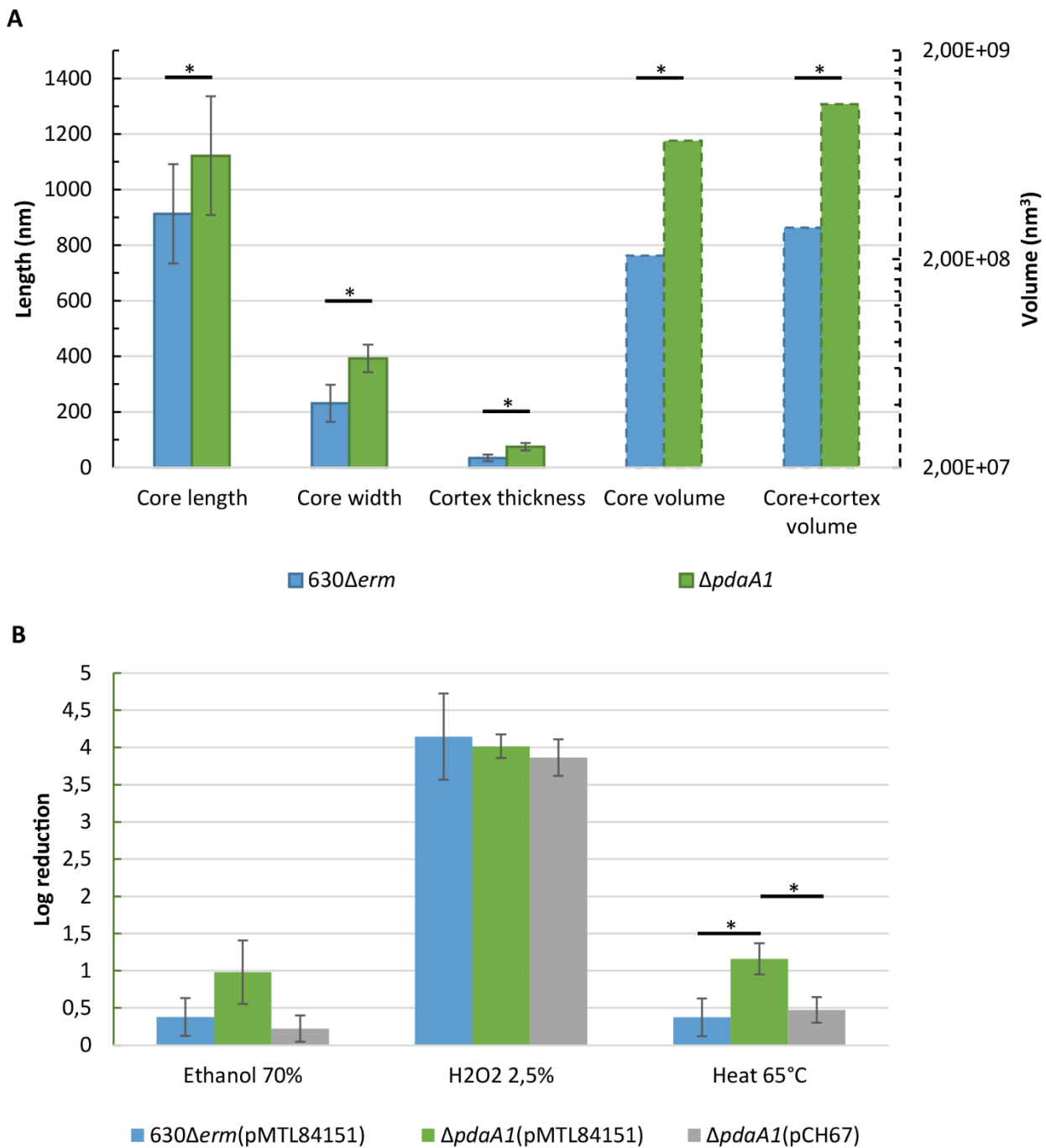


Figure 4. Modification of cortex structure and spore morphology does not alter chemical resistance

Spore measurements (A), obtained for pure spore suspensions of the parental (blue) and *pdaA1* mutant strain (green). Solid bars indicate the measured length (left axis, nm), and the dotted bars indicate the calculated volumes (right axis, nm³). Chemical and heat sensitivity of purified spore suspensions (B), obtained for three independent biological replicates of pure spore suspensions: 630Δerm(pMTL84151) spores in blue, ΔpdaA1(pMTL84151) spores in green and the complemented mutant spores ΔpdaA1(pCH67) strain in grey. * Student test, $p < 0.05$.

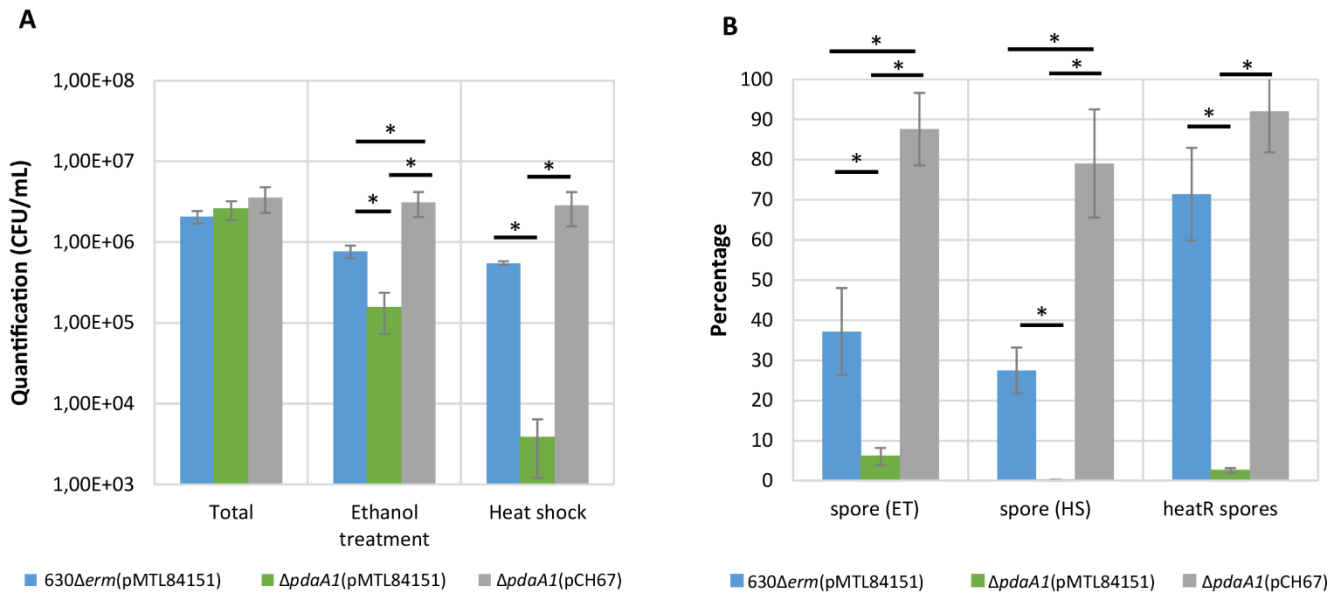


Figure 5 The *pdaA1* mutant has a defect in sporulation and spore heat resistance.

Quantification of sporulation titers after 72h incubation in SM broth (A), percentage of spores recovered after ethanol treatment (ET), heat shock (HS) and heat resistant spores (heat^R) (B) of : 630Δerm(pMTL84151) strain in blue, Δ*pdaA1*(pMTL84151) strain in green and the complemented strain Δ*pdaA1*(pCH67) strain in grey were presented. Results are expressed as the average values and standard deviations of at least three independent experiments. * Student test, $p < 0.005$.

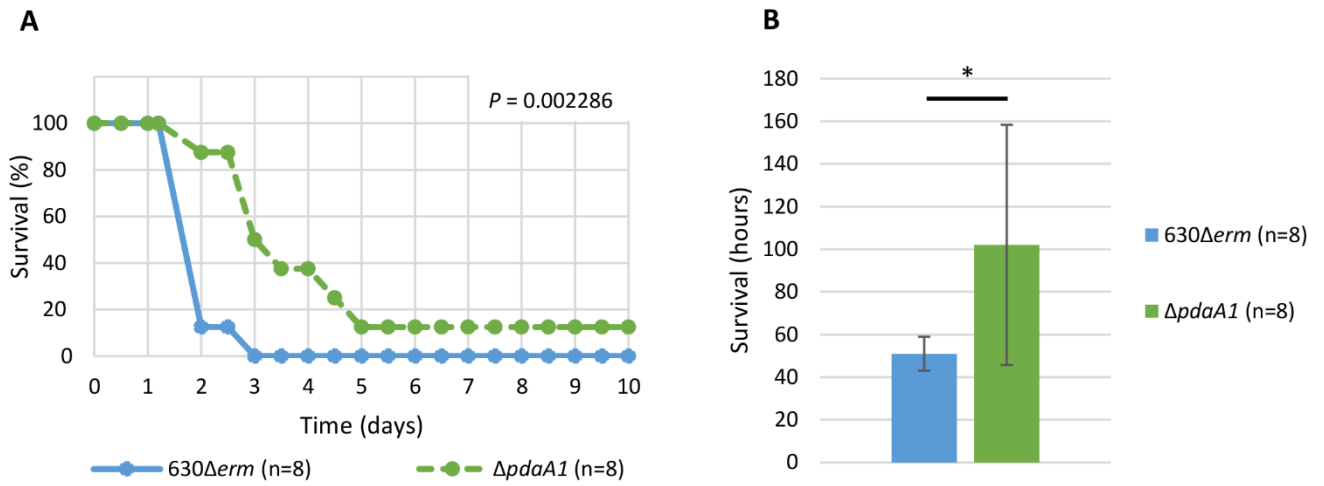


Figure 6. The *pdaA1* mutant strain has a delayed virulence Kaplan-Meier survival curve ($p=0.002286$) depicting hamster survival (A), and average time to mortality (B) for the strain 630 Δ erm in blue and Δ *pdaA1* mutant in green. * Student test, $p < 0,005$

Figure S1. DPA release during germination and quantification of DPA contents of spores

Figure S2. The *pdaA1* mutant and parental strains have a similar growth curve.

Figure S3. Additional germination assays in solid medium

Figure S4. Additional TEM analysis

Figure S5. TEM spore measurements

Figure S6. *pdaA2* mutant has similar germination and sporulation compared to the parental strain.

Table S1. Cortex peaks areas

Table S2. Cortex parameters of the 630 Δ *erm*, the *pdaA1* mutant (Δ 630_14300) and the *pdaA2* mutant (Δ CD630_27190) strains.

Table S3. Identity matrix of PdaA proteins

Table S4. Sporulation titers

Table S5. Cortex analysis yields

Table S6. Primers